Pure Appl. Chem., Vol. 80, No. 8, pp. 1703–1718, 2008.
doi:10.1351/pac200880081703
© 2008 IUPAC

Oxidation-responsiveness of nanomaterials for targeting inflammatory reactions*

Vitaliy V. Khutoryanskiy[1] and Nicola Tirelli[2,‡]

[1]School of Pharmacy, University of Reading, Whiteknights, Reading RG6 6AD, UK; [2]School of Pharmacy and Pharmaceutical Sciences, University of Manchester, Oxford Road, Manchester, M13 9PT, UK

Abstract: Oxidation is an almost ubiquitous feature of inflammatory reactions. We discuss the development of nanocarriers that respond to the presence of oxidants with profound physical reorganization, which could in perspective allow their use for delivering anti-inflammatory principles in an inflammation-responsive fashion. We also present a study demonstrating that the response of polysulfide nanoparticles has a bulk character, i.e., the odixation reactions happen homogeneously throughout the nanoparticles, and not interfacially.

Keywords: nanoparticles; responsiveness; polysulfides; inflammation; oxidation.

INTRODUCTION

This contribution aims to provide (i) a general discussion regarding the need for developing inflammation-responsive carriers (i.e., structures that would allow the delivery active principles in an inflammation-responsive fashion) and (ii) the example of polysulfide-based systems, whose perspective inflammation-responsive character is based on their sensitivity to oxidation, and more specifically of polysulfide nanoparticles, discussing the mechanistic nature of the oxidation reactions.

FIGHTING INFLAMMATION

The four basic descriptors of a situation generically and macroscopically defined as "inflammation", heat (calor), redness (rubor), swelling (tumor), and pain (dolor), have been known and recognized since the dawn of medical sciences (Celsus 30 BC–38 AD). At a tissue level, these cardinal signs correspond to vascular leakage and often angiogenesis (i.e., formation and/or remodeling of often incomplete new blood vessels), that determine swelling of the peripheral tissue and hence nerve compression, and migration from blood circulation of leukocytes, that locally enhance their phagocytic or cytotoxic behavior.

In a general sense, inflammation is a local response to the presence of a foreign body or injury; most commonly, it is possible to define a first phase of response, which is generally referred to as acute inflammation: this is triggered by the actual presence of a foreign object and, ideally, is resolved after its removal: inflammation resolution, in essence, means that both the migration to the peripheral tissue of the inflammatory cells (i.e., the phagocytic and/or cytotoxic leukocytes) and their activity at the site

*Paper based on a presentation at the 41st IUPAC World Chemistry Congress, 5–11 August 2007, Turin, Italy. Other presentations are published in this issue, pp. 1631–1772.

‡Corresponding author: E-mail: nicola.tirelli@manchester.ac.uk

are reduced and eventually silenced because they either die (programmed cell death: apoptosis) or migrate away, possibly through the lymphatic system.

Failure in acute inflammation resolution leads to chronic inflammation, during which, in the most common case, the response changes its target, focusing on endogenous antigens (autoimmune response). The significance of the evolution to chronic inflammation can be appreciated by thinking that these reactions are at the basis of some of the most common pathologies in modern society, such as atherosclerosis [1], rheumatoid arthritis [2], inflammatory bowel disease, multiple sclerosis, cerebral [3] and myocardial ischemia, metabolic disorders such as type 2 diabetes [4], and also a large number of common tumors [5].

Due to the broad spectrum of targets, it is therefore not surprising to see the large number of pharmacological therapies aiming at the interruption of inflammatory pathways or the promotion of those leading to resolution. A short and far from exhaustive list of biological response modifiers must mention compounds that suppress multiple inflammatory genes, such as corticosteroids (steroidal anti-inflammatory drugs), or modulate the activity of inflammatory mediators such as (i) inflammatory cytokines, decreasing their bioavailability (e.g., anti-TNF-α drugs, such as etanercept, or anti-interleukine or anti-TNF-α antibodies, such as infliximab used in rheumatoid arthritis), (ii) enzymes, such as cyclooxygenases or lipooxygenases, involved in the production of inflammatory mediators (e.g., anti-COX-2 drugs, such as a number of nonsteroidal anti-inflammatory drugs), and (iii) enzymes involved in excessive tissue destruction and remodeling, such as matrix metalloproteinases. It is also worth mentioning the attempts of delivery of inflammation-resolving factors, in order, for example, to stimulate the apoptosis of "first-line" inflammatory cells associated to the acute reaction and their rapid phagocytic clearance [6].

These are, in a nutshell, the targets of molecular therapy. Most of the above molecules, however, suffer from non-negligible side effects and, in addition, have relatively low targeting efficiency (i.e., they can influence inflammatory cells also far away from the site of inflammation, while in many cases a local action would be more appropriate). There are also issues related to drug penetration, for example, through multicellular barriers (e.g., blood–brain barrier) or though cell membranes, for which intracellular delivery would be desirable.

Finally, it is also important to note that the control/resolution of inflammatory cell behavior must not completely silence phagocytic behavior, since one important step in the reduction of inflammation is indeed the removal of apoptotic cells from the site [7,8].

The design of carriers that would allow us to selectively target inflammatory cells specifically in an inflamed tissue would be extremely beneficial, since it would not impair the normal trafficking of leukocytes in healthy tissues [9]. On the other hand, comparing the level of sophistication of the molecular design of active molecules and that of carriers, it is apparent that the second one is still in its infancy, with only a few examples still of structures characterized by controlled bioresponsiveness. Additionally, most efforts have been dedicated to target solid tumors, rather than inflammatory reactions; one of the few exceptions, namely, an inflammation-targeting group that has been used to target carrier structures (nanoparticles, liposomes), is folic acid, a molecule for which activated but not resting macrophages overexpress receptors; one must say, however, that folic acid conjugation was originally developed as a tumor-targeting technology and is still mostly used as such.

Among the few other examples of ligands used for directing nanocarriers, one must mention saccharides, which are employed to target selection on macrophage or activated endothelial cell surfaces [10], or mannose or galactose receptors [11]; targeting can also be achieved using antibodies toward cells present in specific areas susceptible to inflammation, such as arterial surfaces [12]. There are also reports of efficacy for less specific ligands (e.g., those binding to integrins), whose internalization is probably quicker in activated macrophages [13].

OXIDATION AND INFLAMMATION

There is an overwhelming body of evidence that inflammatory reactions are almost ubiquitously associated with oxidative stress: the presence of a plethora of highly oxidizing compounds, such as superoxide anion, hydrogen peroxide, hypochlorite (reactive oxygen species, ROS), nitric oxide or peroxinitrite (reactive nitrogen species, RNS), is a common feature of neurodegenerative diseases, such as Parkinson's and Alzheimer's [14], inflammatory bowel diseases, such as Crohn's or ulcerative colitis [15], atherosclerosis [16], inflammatory lung diseases, such as asthma or fibrosis [17], and many others.

The oxidant-producing cascade [18,19] (oxidative burst, summarized in Fig. 1) is generally believed to begin with the activation of NADPH-oxidase, a phagosomal membrane-bound enzyme complex, leading to the production of superoxide anions; this can readily dismutate to hydrogen peroxide, and eventually produce a number of other ROS: for example, hydroxy radicals, from H_2O_2 via Fenton chemistry, and peroxynitrite, from the combination of superoxide with nitric oxide. A key role is also played by myeloperoxidase (MPO), one of the most abundant enzymes in neutrophile granules [20]; MPO is reported to efficiently convert the majority of hydrogen peroxide into hypochlorite, which is likely the major responsibility of the oxidatively cytotoxic behavior of phagocytes [21].

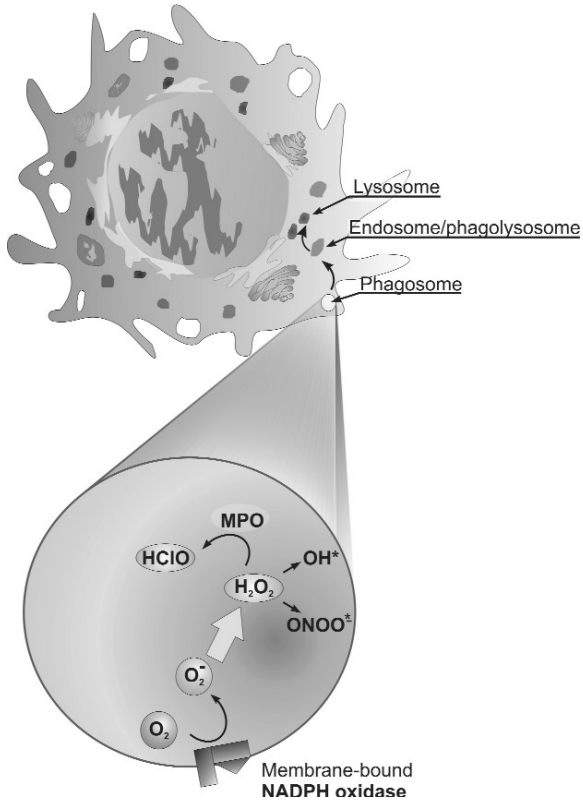

Fig. 1 Pictorial sketch of some of the steps in the cascade of enzymatic events leading to the production of oxidants in vesicular bodies of a macrophage (the same applies to other inflammatory leukocytes). The oxidants can be used intracellularly for the digestion of endocyted bodies, or secreted extracellularly.

These oxidants can be used intracellularly in a phagolysosome for the digestion of a phagocyted foreign body; alternatively, it can be released extracellularly in an oxidative burst that necessarily combines a strong paracrine signal to other inflammatory cells and a diffuse and unspecific cytotoxic effect [22].

As a direct confirmation of the above, antioxidants have been demonstrated to play an important role in anti-inflammatory therapy: most of them decrease vascular permeability and, although they do not necessarily have per se an antiangiogenic effect, they reduce the leukocyte infiltration and thus also inflammation [23].

DEVELOPMENT OF OXIDATION-SENSITIVE CARRIERS

Design criteria

We have tackled the problem of designing inflammation-responsive carrier structures, namely, objects that can possibly deliver complex anti-inflammatory principles at a location of inflammation and at a rate that is proportional to the extent of inflammation, by developing materials that

- can be processed in forms that allow free circulation in body fluids; specifically, their morphology and physicochemical interactions should avoid unspecific accumulation at non-inflamed sites as a result of mechanical entrapment (→ dimensions << 1 μm, to avoid embolization in small capillaries or problematic diffusion in tissues intersititial fluids) or unspecific foreign body reactions, such as uptake by macrophages in non-inflamed areas, leading to their clearance (→ protein-repellent surfaces, to avoid their recognition as foreign bodies which is generally mediated by denaturing protein adsorption). For example, these materials are PEGylated (= surface covered by poly(ethylene glycol) nanoparticles, micelles, or vesicles.
- are sensitive to the presence and concentration of oxidants; the oxidation-induced physicochemical changes (e.g., swelling or solubilization in water) allow much quicker diffusional processes of dispersed molecules (e.g., anti-inflammatory drugs), which result in their release. Eventually, the carrier materials should be eliminated (e.g., through renal excretion) in order to avoid any possible complication arising from their long-term permanence in the host body. This implies that at the end of its life cycle, the carrier should be transformed into low-molecular-weight, water-soluble materials.

Here we will not discuss in detail the possible mechanisms of interaction of oxidation-responsive nanocarriers with (inflammatory) cells, which is the subject of recent and forthcoming publications [24–26], but it is worth mentioning that it is of paramount importance to control endocytic processes (= internalization of the whole carriers in cells), for example, engineering the response of the surface in

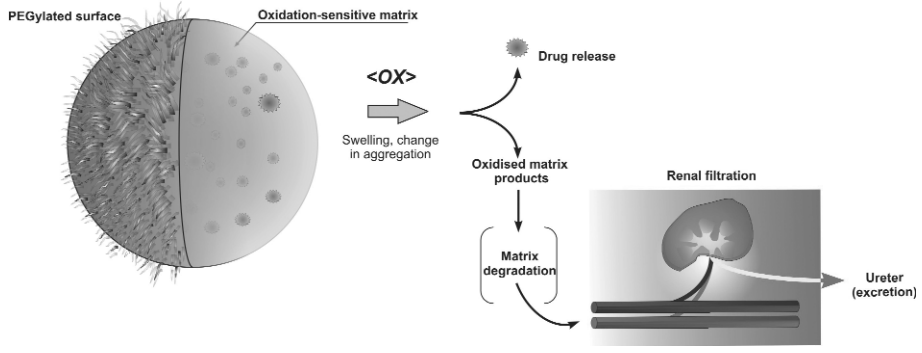

Fig. 2 Schematic mode of action of oxidation-sensitive carriers.

order to provide inflammation-dependent interactions: the effects of a payload can be significantly different if it is released extra- or intracellularly, namely, with or without internalization, since it will mostly affect phagocytic cells in one case, a whole tissue in the other [27].

Chemistry

An ideal REDOX-responsive structure should present at least two oxidation states, stable respectively in reducing and oxidizing physiological conditions and characterized by different aggregation properties. With a water environment in mind, we specifically sought structures that could switch from a hydrophobic, aggregated state to a hydrophilic, soluble, or swellable one, a transition that may determine the release of any matter encapsulated in the aggregate.

Among the tools readily available to the organic chemist, sulfur(II)-containing compounds (sulfides) are likely the best fit to this model, being both hydrophobic and oxidizable to the more polar and hydrophilic sulfoxides or sulfones. Furthermore, the connection of multiple sulfides in a polymeric structure would be advantageous for enhancing cooperative effects and for a good control over mechanical and transport properties; in particular, the sulfur atoms should be linked through short aliphatic chains: polar groups may disfavor hydrophobic aggregation in the reduced state, while long hydrophobic chains would reduce the hydrophilic character of the oxidized products.

We have specifically focused our attention on poly(1,2-alkylene sulfides), which contain only the aforementioned groups [aliphatic chains and sulfur(II)]; these polymers can be oxidized to polysulfoxides or polysulfones, whose hydrophilicity depends on the size of the aliphatic side chain (the group "R" in Fig. 3): the smaller its size, the more dramatic the change in polarity upon oxidation. Unfortunately, poly(ethylene sulfide) (the smallest R group: a hydrogen atom) is a highly crystalline, almost intractable polymer. We have, therefore, focused our attention on poly(propylene sulfide) (PPS),

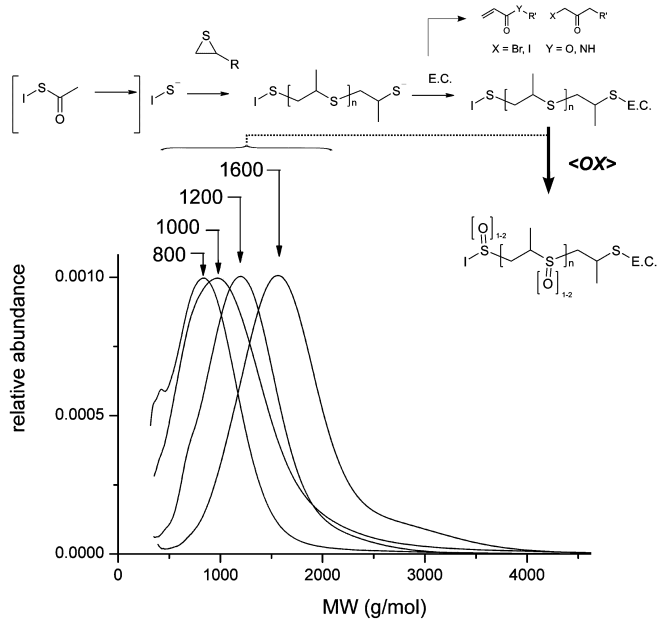

Fig. 3 In the absence of acids or electrophiles (that protonate or react with thiolates) and of oxygen (that oxidizes them to disulfides), termination is virtually absent in episulfide polymerization, i.e., it has a "living" character. Transfer reactions can be completely avoided by using protected thiols to produce initiators ("I" in the scheme) in situ, thus avoiding disulfide impurities.

where "R" is a methyl group; this polymer is completely solubilized in water upon oxidation (e.g., with H_2O_2).

Poly(1,2-alkylene sulfides) are synthesized via "living" anionic ring-opening polymerization of cyclic monomers, the episulfides (Fig. 3); this mechanism allows for a good control over end groups and a narrow dispersity of molecular weights, if impurities such as disulfides (which act as chain transfer agents [28]) are avoided. These advantageous features of episulfide polymerization permit the preparation of polysulfide-containing well-defined block copolymeric [29] or network [30] structures based on small and "monodisperse" polysulfide segments. Indeed, polydispersity indexes routinely lower than 1.2 are obtained also at molar masses < 2000 g/mol, where high polydispersity is a general problem. Upon exposure to oxidants, the polysulfide structure is converted into a polar one containing sulfoxides and/or sulfones. If they are linked together through cleavable bonds, after oxidation the material is indeed converted into small and hydrosoluble materials (i.e., the main requirement for renal excretion).

It is noteworthy that, since the propagating species is a deprotonated thiol (pK_a = 8–9), the presence of water is not necessarily detrimental for the living character of the polymerization; as a result, polysulfides can also be synthesized in a water-rich environment, such as an emulsion [31].

Summary. PPS is an ideal candidate for building oxidation-sensitive carriers, since it is synthesized in a highly controlled fashion (narrow molecular weight dispersion, well-defined terminal groups) and undergoes a hydrophobic-to-hydrophilic transition upon oxidation.

Carrier morphologies

Our group has extensively researched ways to develop PPS-based nanostructures (see design criteria: size << 1 μm) that can be used as oxidation-sensitive carriers, following three main approaches, summarized in Fig. 4:

1. *Polymer synthesis first, then morphogenesis* based on "equilibrium" thermodynamics (= spontaneous self-assembly): well-defined amphiphilic structures (e.g., PEG-PPS block copolymers that combine PEG's protein repellence with PPS responsiveness) can generate a number of self-assembled (lyotropic) structures, whose morphology mostly depends on the volume ratio between the hydrophobic (PPS) and hydrophilic component (PEG) [32]. Therefore, choosing appropriate PEG/PPS ratios, micellar [33] and vesicular [34] objects were produced, allowing, respectively, the encapsulation of hydrophobic and hydrophilic actives (also of macromolecular nature [35]) and their release under oxidative conditions.
2. *Polymer synthesis first, then morphogenesis then chemical curing*: end-functional PPS macromonomers can be dispersed in water by using PEGylated emulsifiers to yield viscous droplets, namely, micro- or miniemulsions whose size and stability can be controlled with the appropriate choice of nature and concentration of the emulsifier; this morphology can later be cured through free radical polymerization, yielding stable and cross-linked nanoparticles [36]. Please note that curing is necessary, because due to their low T_g, the polysulfides in emulsion form viscous droplets, which are poorly stable against coalescence.
3. *Morphogenesis first, then all synthetic operations*, comprising curing: the hydrophobic episulfides (i.e., the monomers used in PPS synthesis) can be emulsified too by the use of PEGylated amphiphiles, and the resulting emulsions can be polymerized and then cross-linked, thus performing together the two stages of point 2 [37].

We will now specifically focus on strategy III, namely, on PPS nanoparticles obtained through emulsion polymerization and cross-linking of propylene sulfide. This preparative method is very convenient because it minimizes the number of purification and characterization, since morphogenesis and chemical operations are conducted *one pot* (Fig. 5): in the same environment, multifunctional thioacetates are deprotected, to uncover thiolates, and emulsified with monomers, to yield star-shaped polysulfides; they are therefore cured by linking together the polysulfide terminal thiolates either by dimer-

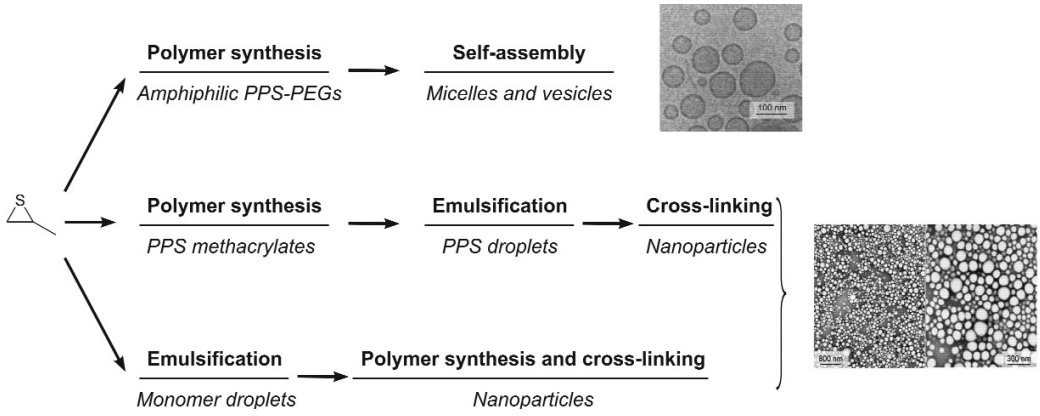

Fig. 4 Scheme of the different preparative strategies for polysulfide nanocarriers.

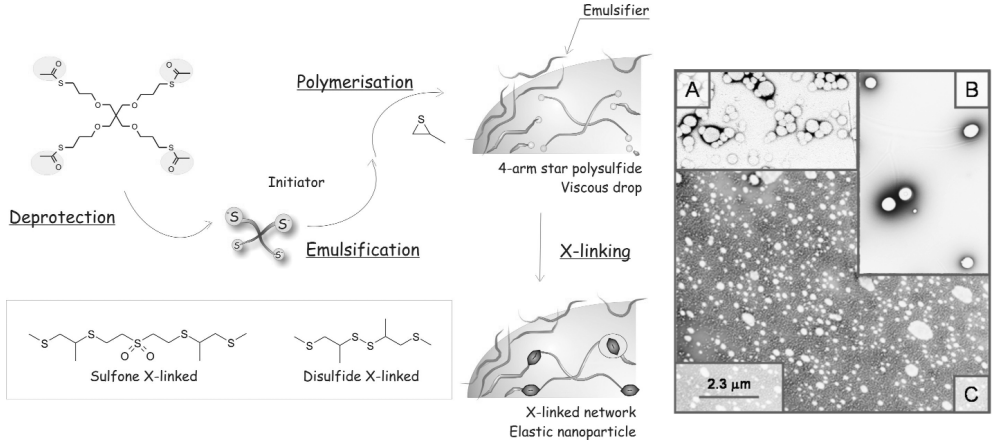

Fig. 5 Scheme of the preparative steps of method III leading to cross-linked polysulfide nanoparticles. The cross-links are based on sulfones (particles ***A***), 50:50 sulfones/disulfides (particles ***B***) or disulfides (particles ***C***).

izing them in the form of disulfides, or by reacting them with difunctional reagents, such as diacrylates or a divinyl sulfone [37].

The emulsifier used in the polymerization (Pluronic F127) is permanently retained on the nanoparticle surface, in this way providing a permanent PEGylation.

Mechanism of responsiveness for polysulfide nanoparticles: Surface or bulk?

Polysulfide nanoparticles are designed to host an active principle and release it in the presence of oxidants that convert the hydrophobic polysulfide matrix into hydrophilic and water-swollen polysulfoxides/polysulfones. The validity of this approach has been verified, for example, enzymatically generating in situ the oxidizing species that trigger the release [38].

Until now, however, it has never been completely clarified whether the reaction proceeds with a predominantly bulk or a surface mechanism, namely, whether the balance between reaction speed and diffusion in the matrix leans toward homogeneous reaction throughout the polysulfide matrix (diffusion quicker than reaction) or toward interfacial reaction at its surface (reaction quicker than diffusion). These two limiting situations correspond to:

- *Different overall reaction kinetics*: If the reaction is interfacial, for an extended period of time the hydrophobe/hydrophile interface has no large variation; therefore, the amount of residual thioether decreases roughly linearly with time (the number of groups oxidized in the time unit is roughly constant). If the reaction has a bulk mechanism, it should show a classical autoacceleration pattern: most oxidants are polar and hydrophilic molecules, scarcely soluble in the initial polysulfide matrix, but increasingly soluble with increasing degree of oxidation; the increase in oxidant concentration should thus correspond to an increase in reaction rate. We expect, therefore, the residual thioether to decrease in a sigmoidal fashion, with an initial lag time inversely proportional to the solubility of the oxidants in the polysulfide matrix.
- *Different release profiles (Fig. 6)*: A drug dispersed in a matrix undergoing a bulk swelling would likely show a release time profile with a sigmoidal shape: little release from a hydrophobic matrix, but first order-like release (release rate exponentially decreasing with time) when this becomes hydrophilic enough to allow long-range diffusion. On the contrary, a zero order-like release profile (release rate roughly independent on time) will be exhibited in the case of surface oxidation.

NOTE: The characteristic dimensions of the material (the nanoparticle) play a major role in defining the nature of the response: at a 100-nm scale, a reaction can proceed with a bulk mechanism because a short time is required for the diffusion of a reactand through such short distances, while the diffusion of the same molecule through the same materials at a mm scale can be too slow for the reaction to take place. It is therefore important to note that a bulk oxidation mechanism for nanoparticles does not imply the same to happen for a macroscopic object.

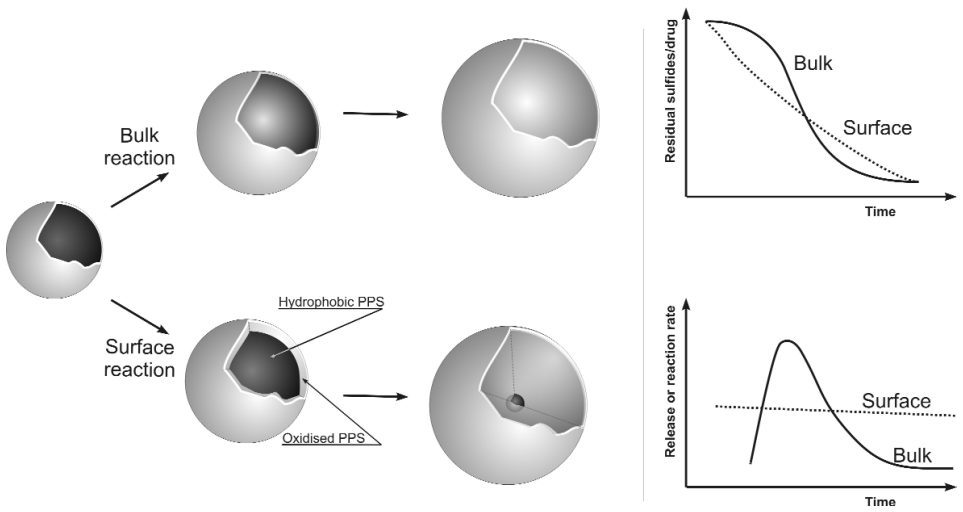

Fig. 6 During oxidation, the polysulfide nanoparticles are expected to swell because of water ingress into an increasingly hydrophilic matrix; this can happen homogeneously throughout the nanoparticle core (bulk reaction) or interfacially moving from the periphery to the center (surface reaction). In the first case, the reaction will autoaccelerate, due to the increasing concentration of polar oxidants in the increasingly swollen material. Release processes would closely follow the nanoparticle swelling, if diffusion from the cross-linked polysulfide matrix is avoided.

Polysulfide nanoparticles significantly scatter visible light, since PPS' refractive index is markedly different from that of water (1.590 vs. 1.332, respectively). Upon exposure to hydrogen peroxide used as model oxidizing agent, they become increasingly less opaque and eventually completely transparent (Fig. 7).

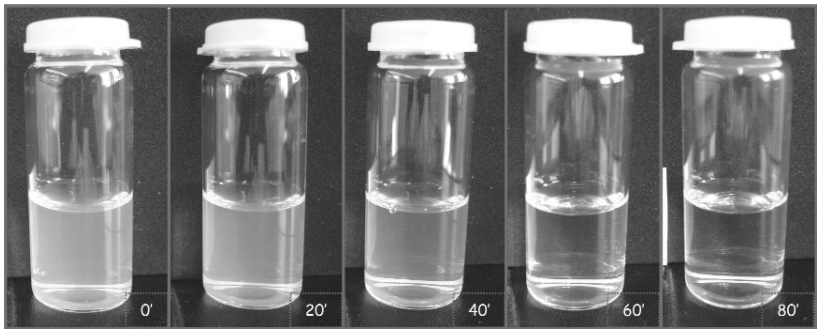

Fig. 7 Opacity of polysulfide nanoparticles (disulfide cross-linked; average size: 240 nm, conc. 0.35 % wt) exposed to 10 % H_2O_2 as a function of time.

Turbidity could be a convenient method to follow the oxidation kinetics, although its relationship with molecular events may be complex; however, we are reasonably confident, assuming the optical density of the suspensions to be directly related to the sulfide content, since:

- With optical densities <1.5, the dispersion turbidity is roughly linear with nanoparticle concentration, both before and during oxidation; this ensures that multiple scattering is not tremendously significant and turbidity data can, therefore, be used for further calculations.
- Turbidity depends on concentration, size, and refractive index of the nanoparticles; however, if cleavable groups (e.g., hydrolyzable bonds) are absent, there is no reason for the nanoparticle number concentration to change during oxidation. Therefore, we can assume the variables affecting turbidity to be only refractive index and size.
- If the nanoparticles roughly double in size, they have an 8-fold volume increase, corresponding to a roughly 1:7 polymer/water volume ratio. PPS has a reported refractive index of 1.590; its oxidation products may have slightly higher values, but not larger than 1.7 (aromatic polysulfones); therefore, for such a volume ratio, a linear combination with the refractive index of water (roughly 1.34) would provide a value of 1.37–1.38. The variation in refractive index due to swelling is, therefore, large and should determine a strong decrease in turbidity.
- IR absorbance of sulfoxides (S=O stretching vibration peaked at 1030 cm^{-1}, normalized with respect to the methyl bending vibration at 1415 cm^{-1}) closely follows the time dependence of the turbidity signal (Fig. 8).
- Dynamic light-scattering data show that the nanoparticles roughly double in radius upon oxidation, a phenomenon which should increase turbidity (Fig. 8); however, from a qualitative point of view, this contribution appears to be negligible, since turbidity shows exactly the opposite behavior.

From the above points, we conclude that turbidity, although probably mostly related to the swelling extent in water, provides a reliable indication of the extent of polysulfide oxidation.

All curves in Fig. 8, as well as those obtained at different temperatures and using different amounts of hydrogen peroxide (Fig. 9), show clear sigmoidal shapes, which, being generally related to autoaccelerating reaction, suggest a bulk oxidation mechanism, namely, the oxidants diffuse more rapidly than they react.

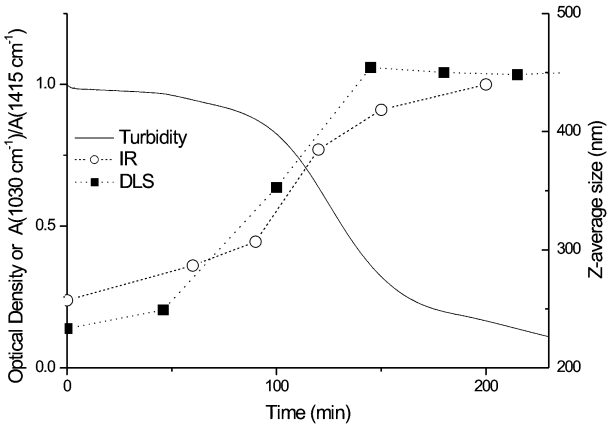

Fig. 8 The decrease in turbidity (solid line) follows a parallel path to the relative increase in sulfoxide content (open circles). The increase in nanoparticle dimensions due to swelling (solid squares) should produce an opposite trend in turbidity (increased scattering from larger particles); since this is not recorded, we conclude that the effect of changes in refractive index overwhelm that of changes in dimension. 1:1 disulfide/sulfone cross-linked nanoparticles; conc. 0.35 % wt.

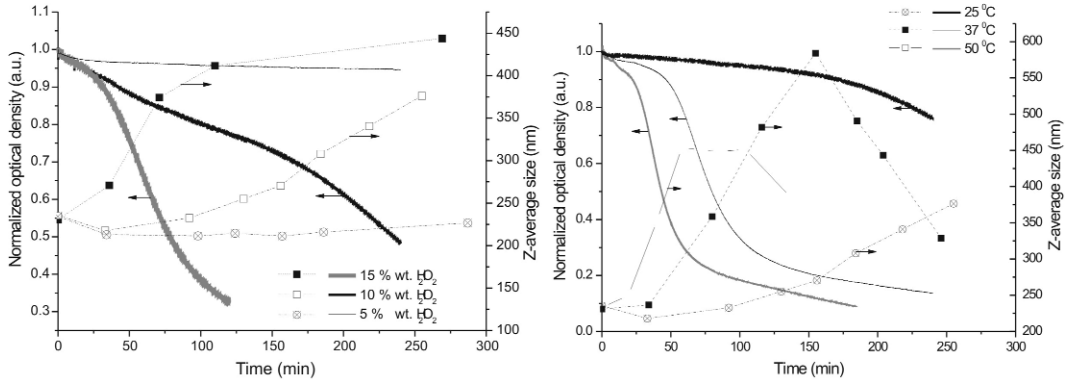

Fig. 9 Turbidity and dimensions of nanoparticle dispersions as a function of increasing hydrogen peroxide concentration and temperature, which obviously speed up the oxidation reaction. 1:1 disulfide/sulfone cross-linked nanoparticles; conc. 0.35 % wt; left: T = 50 °C, right: H_2O_2 conc. = 10 % wt.

For a further confirmation, we have compared polysulfide nanoparticles cross-linked with disulfides or sulfones: these two chemical groups have markedly different polarities, and, therefore, polar molecules, such as hydrogen peroxide, should be substantially more soluble in a sulfone cross-linked matrix. This should have a dramatic influence for a bulk reaction mechanism, increasing the initial reaction rate and therefore also reducing the lag time. Indeed, this behavior is observed, with an increasing reaction rate obtained by increasing the proportion of sulfones present as cross-linking groups (Fig. 10).

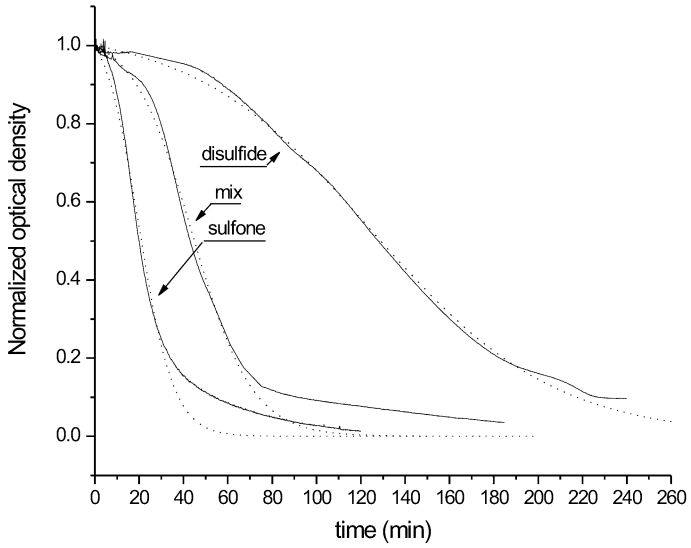

Fig. 10 Turbidity curves obtained from the exposure of polysulfide nanoparticles obtained by cross-linking the terminal thiolates of 4-armed star polysulfide chains 100 % with disulfides, 100 % with sulfones or with a 1:1 sulfone/disulfide mixture (T = 50 °C, right: H_2O_2 conc. = 10 % wt.)

In principle, it is possible to obtain semiquantitative data by fitting the data with a kinetic model that takes into account the dependence of the oxidant concentration in the organic matrix. In doing that, we will assume:

a. a bimolecular reaction mechanism that involves one sulfide group and one molecule of hydrogen peroxide [39,40]; this situation should translate into a second-order reaction kinetics

$$\frac{d[S]}{dt} = -k'[S][\mathrm{H_2O_2}]_{\mathrm{loc}} = -k'[S]P[\mathrm{H_2O_2}]_{\mathrm{tot}} \tag{1}$$

where the local concentration of hydrogen peroxide in the polysulfide domain, $[H_2O_2]_{loc}$, depends on its concentration in the water phase $[H_2O_2]_{tot}$ through a partition coefficient P.

b. that, due to the large excess of oxidant used in our experiment, $[H_2O_2]_{tot}$ is constant throughout the duration of the experiments.

c. that at time $t = 0$, $[H_2O_2]_{loc} = P_0[H_2O_2]_{tot}$ where P_0 is the water/polysulfide partition coefficient (which is matrix-specific, i.e., it is different in disulfide or sulfone cross-linked matrices, because it depends on the matrix polarity), while at time $t = \infty$, $[H_2O_2]_{loc} = [H_2O_2]_{tot}$. Having set the limits, the time dependence of $[H_2O_2]_{loc}$ is still unknown. We further assume, for ease of calculation, that during oxidation, $[H_2O_2]_{loc}$ will increase linearly with the polarity of the matrix, which on its turn is linearly related to the degree of oxidation:

$$\begin{aligned}
[\mathrm{H_2O_2}]_{\mathrm{loc}}(t) &= P(t)[\mathrm{H_2O_2}]_{\mathrm{tot}} = \{P_0(1-\frac{[S]_0-[S](t)}{[S]_0})+\frac{[S]_0-[S](t)}{[S]_0}\}[\mathrm{H_2O_2}]_{\mathrm{tot}} \\
[\mathrm{H_2O_2}]_{\mathrm{loc}}(t) &= \{P_0-\frac{[S](t)}{[S]_0}(1-P_0)\}[\mathrm{H_2O_2}]_{\mathrm{tot}}
\end{aligned} \tag{2}$$

By combining eqs. 1 and 2, one obtains an expression for the reaction rate that is no longer simply linear in [*S*], but takes the form of a logistic equation:

$$\frac{d[S]}{dt} = -k'[S]\{P_0 - \frac{[S](t)}{[S]_0}(1-P_0)\}[H_2O_2]_{tot} = -k'[H_2O_2]_{tot}(P_0[S] - \frac{(1-P_0)}{[S]_0}[S]^2) \quad (3)$$

The integration of eq. 3 provides a sigmoidal analytical expression of [*S*](*t*):

$$[S](t) = \frac{P_0[S]_0}{(2P_0-1)e^{k'P_0[H_2O_2]_{tot}t} + 1 - P_0} = \frac{A}{B + e^{Ct}} \quad (4)$$

It is noteworthy that (i) turbidity and sulfide concentration are related through an unknown proportionality constant, which, when fitting turbidity data, will be embedded in the value of constant A, (ii) small differences in the experimental conditions (timing of the addition of hydrogen peroxide, precise concentration of the nanoparticles, …) may result in the presence of corrective constants: this is the case of hydrogen peroxide concentration, which, for example, at high temperature may decrease because of spontaneous decomposition. In fitting the turbidity data, therefore, we have focused our attention only on the time-dependent part of the equation, that is the coefficient $C = k' P_0[H_2O_2]_{tot}$.

The results (Table 1) show that *C* depends both on temperature (which influences both kinetic constant and solubility of H_2O_2) and on hydrogen peroxide concentration. However, the dependence on $[H_2O_2]_{tot}$ does not appear to be linear, as it would be on the basis of a bimolecular reaction mechanism: the *C* values obtained at different temperatures fall roughly on the same plot only when divided by the square of $[H_2O_2]_{tot}$ (Fig. 11), therefore indicating a quadratic dependence.

Table 1

Sample	Cross-linking	$[H_2O_2]$, %	Temperature, °C	1/C (min)
B_15_50	1:1 sulfone/disulfide	15	50	3.9
B_15_37	1:1 sulfone/disulfide	15	37	11.1
B_15_25	1:1 sulfone/disulfide	15	25	21.5
B_10_50	1:1 sulfone/disulfide	10	50	16.4
B_10_37	1:1 sulfone/disulfide	10	37	21.1
B_10_25	1:1 sulfone/disulfide	10	25	108
B_5_50	1:1 sulfone/disulfide	5	50	40.4
B_5_37	1:1 sulfone/disulfide	5	37	119
B_5_25	1:1 sulfone/disulfide	5	25	318
A_10_50	100 % sulfone	10	50	7.9
C_10_50	100 % disulfide	10	50	40.9

The fitting results, therefore, confirm that the sigmoidal turbidity curves obtained upon exposure of the nanoparticle dispersions to hydrogen peroxide can be associated to an autoaccelerating oxidation, i.e., to a bulk reaction and not to an interfacial one. However, the molecular mechanism seems to be more complex than a simple bimolecular reaction.

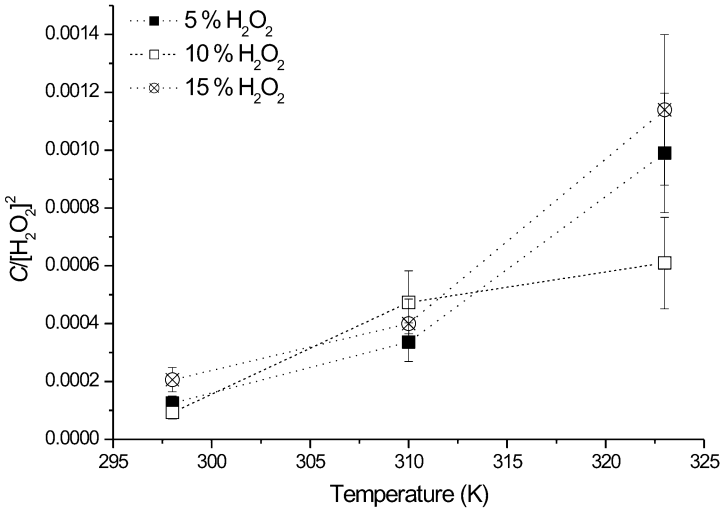

Fig. 11 Within the experimental error, which is quite high for room temperature oxidation, the parameter C (see eq. 4) becomes substantially independent on hydrogen peroxide concentration only when divided by its square. The dependence on temperature arises from both the kinetic constant and the partition coefficient.

EXPERIMENTAL

Preparation of nanoparticles

Activation of the initiator and polymerization: 0.25 g of Pluronic F-127 was dissolved in 25 mL (2 % w/v) of degassed, double-distilled, and filtered water in a 100-mL three-neck, round-bottom flask. The system was continuously stirred at 1000 rpm and purged with nitrogen for 10 min before polymerization. Propylene sulfide (1.0 mL, 0.946 g, 12.8 mmol) was then added. 0.0768 g (0.14 mmol) of pentaerythritol tetrathioester were separately mixed with 1.02 mL of 0.5 M methanol solution of sodium methanoate under nitrogen atmosphere. The disappearance of ν(C=O) thioester band at 1687 cm^{-1} and appearance of the band at 1631 cm^{-1} in Fourier transform infrared (FTIR) spectrum confirmed the cleavage of the thioester groups. The resulting methanol solution was added to the emulsified monomer and stirred for 10 min.

The deprotected initiator was then added to the polymerization mixture, followed by 0.15 mL of diaza[5.4.0]bicycloundec-7-ene (DBU) in 8:1 molar ratio with the thioester. The reaction mixture was stirred under inert conditions for 2 h and then was exposed to cross-linking.

Cross-linking: Nanoparticles A were cross-linked by adding 0.026 mL of divinyl sulfone dissolved in 0.25 mL dichloromethane (1:2 molar equiv to thioester), stirring this mixture overnight under nitrogen prior to purification. The bridges between tetra-armed macromolecules all contain sulfones.

Nanoparticles B were cross-linked by adding 0.013 mL of divinyl sulfone dissolved in 0.25 ml of dichloromethane (1:1 molar equiv to thioester), stirring this mixture for 2 h under nitrogen, then bubbling air through the reaction mixture for 5 min and continuing the stirring overnight prior to purification. The bridges between tetra-armed macromolecules are roughly 50 % based on sulfone groups and 50 % on disulfide bonds (a variable amount of free thiols, up to 10 %, could still be detected after purification, using Ellman's reagent; we assume, however, them to slowly disappear upon storage).

Nanoparticles C were cross-linked by bubbling air through the reaction mixture for 5 min, stirring the reaction mixture under air overnight prior to purification. The connections between tetra-armed polymer chains are all based on disulfide bonds (again small amounts of free thiols could still be detected after purification).

Purification: The nanoparticles dispersions were first extracted with 2 portions of dichloromethane (5 mL), then purified through dialysis through 15 kDa membranes (Spectrum Laboratories, USA) against 1 L of water (6 changes during 48 h) and then ultrafiltration in stirred cells (Amicon system) through 300 kDa membranes (Millipore, USA). The nanoparticle concentration was gravimetrically determined after removal of water by freeze drying.

Oxidation of nanoparticles

Appropriate volumes of nanoparticles dispersions in water (0.1–1.0 ml at a roughly constant concentration of 3.5 mg/ml = 0.35 % wt) were added to a fixed volume (10 mL) of aqueous solutions of hydrogen peroxide of chosen concentration and at a controlled temperature and analyzed spectrophotometrically or through dynamic light scattering.

Physicochemical characterization

The changes in optical density of nanoparticle dispersions upon oxidation were monitored with UV/vis spectrophotometer Perkin Elmer Lambda 25 at 600 nm using UV WinLab software. The temperature of these experiments was kept constant using PTP-6 Peltier system. The z-average size and size distributions of nanoparticles were measured with the help of Zetasizer Nano ZS Instrument (Model ZEN2500, Malvern Instruments, UK).

FTIR: The infrared spectra were recorded using Tensor 27 Fourier Transform Infrared Spectrophotometer (Bruker) equipped with MKII Golden GateTM Single Reflection ATR system (Specac) and 3000 SeriesTM High Stability Temperature Controller with RS232 Control (Specac). The spectra of nanoparticles upon oxidation in hydrogen peroxide solutions were recorded after placing a drop of the reaction mixture on a Golden Gate Heated Diamond ATR Top-Plate and complete evaporation of water at 50 °C.

Transmission electron microscopy: The nanoparticle dispersions were pipetted on carbon/formvar coated copper 100 mesh grids for 2–3 min, then the grids were washed in distilled water 3 times, stained in 1 % uranyl acetate in distilled water and air dried. Samples were observed in Technai 12 electron microscope at 100 kV.

CONCLUSIONS

The sensitivity to oxidation exhibited by polysulfide-based nanocarriers is an interesting feature for a perspective targeting of inflammatory reactions. Using hydrogen peroxide as a model oxidant, we have here investigated some elements useful for clarifying the mechanism of oxidation of cross-linked polysulfide nanoparticles. At a material level, the response is based on the increase in polarity of the polymer matrix and on its corresponding swelling with water; from the kinetic analysis of the reaction, which show a typical autoaccelerating behavior, we have evidence that the reaction has a bulk character and therefore proceeds homogeneously through the particles. At a molecular level, it seems that a bimolecular mechanism is not sufficient to describe the reaction, while more (possibly two) hydrogen peroxide molecules are likely involved; as a consequence, the dependence of the reaction rate on oxidant concentration is likely not linear, which could be beneficial for responding only to high concentrations of oxidants, i.e., only to strong inflammation.

ACKNOWLEDGMENTS

BBSRC is gratefully acknowledged for financial support (grant no. BBS/B/01537). NT is indebted to EPSRC for an Advanced Research Fellowship.

REFERENCES

1. P. Libby. *Nature* **420**, 868 (2002).
2. D. M. Lee, M. E. Weinblatt. *Lancet* **358**, 903 (2001).
3. F. C. Barone, G. Z. Feuerstein. *J. Cereb. Blood Flow Metab.* **19**, 819 (1999).
4. G. S. Hotamisligil. *Nature* **444**, 860 (2006).
5. A. Mantovani. *Nature* **448**, 547 (2007).
6. D. W. Gilroy, T. Lawrence, M. Perretti, A. G. Rossi. *Nature Rev. Drug Discov.* **3**, 401 (2004).
7. R. S. Scott, E. J. McMahon, S. M. Pop, E. A. Reap, R. Caricchio, P. L. Cohen, H. S. Earp, G. K. Matsushima. *Nature* **411**, 207 (2001).
8. C. Ward, I. Dransfield, E. R. Chilvers, C. Haslett, A. G. Rossi. *Trends Pharmacol. Sci.* **20**, 503 (1999).
9. A. D. Luster, R. Alon, U. H. von Andrian. *Nature Immunol.* **6**, 1182 (2005).
10. C. Ehrhardt, C. Kneuer, U. Bakowsky. *Adv. Drug Delivery Rev.* **56**, 527 (2004).
11. F. Chellat, Y. Merhi, A. Moreau, L. Yahia. *Biomaterials* **26**, 7260 (2005).
12. P. I. H. de Bittencourt, D. J. Lagranha, A. Maslinkiewicz, S. M. Senna, A. M. V. Tavares, L. P. Baldissera, D. R. Janner, J. S. Peralta, P. M. Bock, L. L. P. Gutierrez, G. Scola, T. G. Heck, M. S. Krause, L. A. Cruz, D. S. P. Abdalla, C. J. Lagranha, T. Lima, R. Curi. *Atherosclerosis* **193**, 245 (2007).
13. J. Qin, D. W. Chen, H. Y. Hu, Q. Cui, M. X. Qiao, B. Y. Chen. *Chem. Pharm. Bull.* **55**, 1192 (2007).
14. J. Emerit, A. Edeas, F. Bricaire. *Biomed. Pharmacother.* **58**, 39 (2004).
15. M. L. Harris, H. J. Schiller, P. M. Reilly, M. Donowitz, M. B. Grisham, G. B. Bulkley. *Pharmacol. Ther.* **53**, 375 (1992).
16. M. Navab, G. M. Ananthramaiah, S. T. Reddy, B. J. Van Lenten, B. Ansell, G. C. Fonarow, K. Vahabzadeh, S. Hama, G. Hough, N. Kamranpour, J. A. Berliner, A. Lusis, A. M. Fogelman. *J. Lipid Res.* **45**, 993 (2004).
17. I. Rahman, W. MacNee. *Eur. Respir. J.* **16**, 534 (2000).
18. M. B. Hampton, A. J. Kettle, C. C. Winterbourn. *Blood* **92**, 3007 (1998).
19. J. B. Park. *Exp. Mol. Med.* **35**, 325 (2003).
20. D. F. Bainton, J. L. Ullyot, M. G. Farquhar. *J. Exp. Med.* **134**, 907 (1971).
21. B. M. Babior. *Am. J. Med.* **109**, 33 (2000).
22. H. Jaeschke. *Proc. Soc. Exp. Biol. Med.* **209**, 104 (1995).
23. R. M. Touyz, E. L. Schiffrin. *Histochem. Cell Biol.* **122**, 339 (2004).
24. S. T. Reddy, A. J. van der Vlies, E. Simeoni, V. Angeli, G. J. Randolph, C. P. O'Neill, L. K. Lee, M. A. Swartz, J. A. Hubbell. *Nature Biotechnol.* **25**, 1159 (2007).
25. S. T. Reddy, A. Rehor, H. G. Schmoekel, J. A. Hubbell, M. A. Swartz. *J. Controlled Release* **112**, 26 (2006).
26. A. Rehor, H. Schmoekel, N. Tirelli, J. A. Hubbell. *Biomaterials* **29**, 1958 (2008).
27. N. Tirelli. *Curr. Opin. Colloid Interface Sci.* **11**, 210 (2006).
28. G. Kilcher, L. Wang, N. Tirelli. *J. Polym. Sci., Part A, Polym. Chem.* **46**, 2233 (2008).
29. A. Napoli, N. Tirelli, G. Kilcher, J. A. Hubbell. *Macromolecules* **34**, 8913 (2001).
30. G. Kilcher, L. Wang, C. Duckham, N. Tirelli. *Macromolecules* **40**, 5141 (2007).
31. A. Rehor, N. Tirelli, J. A. Hubbell. *Macromolecules* **35**, 8688 (2002).
32. A. Napoli, N. Tirelli, E. Wehrli, J. A. Hubbell. *Langmuir* **18**, 8324 (2002).
33. L. Wang, G. Kilcher, N. Tirelli. *Macromol. Biosci.* **7**, 987 (2007).
34. A. Napoli, M. Valentini, N. Tirelli, M. Muller, J. A. Hubbell. *Nat. Mater.* **3**, 183 (2004).
35. A. Napoli, M. J. Boerakker, N. Tirelli, R. J. M. Nolte, N. A. J. M. Sommerdijk. *Langmuir* **20**, 3487 (2004).
36. G. Kilcher, C. Duckham, N. Tirelli. *Langmuir* **23**, 12309 (2007).

37. A. Rehor, J. A. Hubbell, N. Tirelli. *Langmuir* **21**, 411 (2005).
38. A. Rehor, N. E. Botterhuis, J. A. Hubbell, N. A. J. M. Sommerdijk, N. Tirelli. *J. Mater. Chem.* **15**, 4006 (2005).
39. D. Barnard, L. Bateman, J. L. Cuneen. In *The Chemistry of Organic Sulfur Compounds*, N. Kharasch, C. Y. Meyers (Eds.), Pergamon Press, New York (1961).
40. T. H. Nguyen, J. Burnier, W. Meng. *Pharm. Res.* **10**, 1563 (1993).